applied optics

Developing an integrated photonic system with a simple beamforming architecture for phased-array antennas

Weimin Zhou,[1,*] Michael Stead,[1] Steven Weiss,[1] Olukayode Okusaga,[2] Lingjun Jiang,[3] Stephen Anderson,[1,3] and Z. Rena Huang[3]

[1]US Army Research Laboratory, Sensors & Electron Devices Directorate, 2800 Powder Mill Road, Adelphi, Maryland 20783, USA
[2]Johns Hopkins University, Applied Physics Laboratory, Laurel, Maryland 20723, USA
[3]Rensselaer Polytechnic Institute, Electrical, Computer and System Engineering Department, Troy, New York 12180, USA
*Corresponding author: weimin.zhou.civ@mail.mil

Received 8 July 2016; revised 11 August 2016; accepted 12 August 2016; posted 15 August 2016 (Doc. ID 269999); published 22 September 2016

We have designed a simplified true-time-delay beamforming architecture using integrated photonics for phased-array antennas. This architecture can independently control multiple RF beams simultaneously with only a single tuning parameter to steer the beam in each direction for each beam. We have made a proof-of-the-principle demonstration of an X-band, 30 × 4-elements, fiber-optics-based beamformer for one-dimensional steering in transmission mode. The goal is to develop a semiconductor-based integrated photonic circuit so that a 2D beamforming array for both transmit and receive operations can be made on a single chip. For that, we have designed a Si-based integrated waveguide circuit using two types of "slow-light" waveguide for tunable time delays for two-dimensional steering.

OCIS codes: (060.5625) Radio frequency photonics; (130.3120) Integrated optics devices; (130.0130) Integrated optics; (060.2360) Fiber optics links and subsystems; (060.3735) Fiber Bragg gratings.

http://dx.doi.org/10.1364/AO.56.0000B5

1. INTRODUCTION

Phased-array antennas have been widely used in both military platforms and commercial radio-frequency (RF) systems. By programming a phase variation in each element of an antenna array, one can steer the transmission or reception angle for a collimated beam. Therefore for an N-element phased array, N different phases have to be programmed to form the beam for each steering angle [1]. With the recent advancement of digital technology, RF waveforms can be digitally produced and converted to an analog RF signal for transmission with the antenna; therefore, digital beamforming can be also realized by digitally programming a phase delay for the waveform for each antenna element [2,3]. However, in wideband and high-frequency applications, this technology is severely limited. First, since the phase is a function of frequency, phase-shifters-based phase array antenna do not have a perfectly linear phase-frequency characteristic, which will cause deformation for a wideband RF signal waveform [4]. Second, the system may require a processing rate of the order of hundred terabytes per second. Even with the most advanced digital systems, the amount of digital processing at such high frequencies cannot be done with reasonable size, weight, and power consumption nor with reasonable computation time. High-frequency performance is also limited by the digital clock's jitter.

At US Army Research Laboratory (ARL), we are developing phased-array antenna technology using RF photonics for the next-generation Radar system. RF photonic systems offer ultrawide bandwidth and low-loss time delay lines, which may provide the critical elements for an optically controlled beamforming phased-array antenna with optical true-time delays (TTDs). Since the early 90s, many optical TTD schemes for beamforming have been proposed and studied [5–12]. However, two major problems remain. One is performance, such as poor spurious free dynamic range (SFDR) and system loss in the RF photonic link. Another is the high cost for realistic large array system implementation. Recently, there has been significant improvement in RF photonic links, which demonstrate RF-to-RF link gain with high SFDR [13]. Driven by the telecommunications industry, the costs of commercial photonic devices have dropped significantly, which is beneficial for RF photonic systems. However, for an $1 \times N$ element array with K steering positions, most of these systems require a fixed wavelength laser with a $1 \times N$ beam splitter and an optical switch matrix to make N times K fixed optical time delay. Or a system using a fiber grating to generate discrete time

delays requires a wavelength-tunable laser and $1 \times N$ beam splitters, and K gratings per emitter element for a total of N times K gratings [12]. Adding a second dimension to the array ($M \times N$) increases the requirements dramatically. It increases the number of elements to $M \times N$, and increases the number of gratings per element to $K \times J$, where J is the number of steering positions in the second dimension. For a typical phased-array antenna with 1000 elements and 10,000 discrete steering positions, these types of systems will easily require more than a million components to be built. Since most current photonic devices are not monolithically integrated, the system would be very complex to build and therefore expensive, large in size, and have high power consumption. At ARL, we have designed a simplified architecture for the TTD beamformer to solve this problem by significantly reducing the number of devices needed.

In this paper, we present our efforts of design and demonstration of a simplified photonic beamforming architecture for phased-array antenna design. We also present our development of a semiconductor integrated photonic system toward a future chip-scale phased-array antenna beamformer. In Section 2, we present the design and development of our photonic controlled phased-array antenna system architecture, by first reviewing beamforming principles in Section 2.A, and earlier work using free-space optics in Section 2.B. Building on this work, we detail the system design using fiber-optic devices in Section 2.C. In Section 2.D, we discuss our architecture design and concept for transmit and receive operations on a single system, and follow with Section 2.E, describing a our multiple-beam antenna design, which allows the system to engage in simultaneous and independent control of multiple RF beams. Section 3 details the experimental demonstration of the fiber-optic system, with simulations of a fiber-Bragg-grating-based tunable time delay beam steering from Section 3.A compared with experimental results in Section 3.B. Together, Sections 2 and 3 demonstrate a proof of concept of the optical circuit architecture. Section 4 details how this concept can be realized as an integrated photonic TTD array circuit for use in a chip-scale beamformer for two-dimensional (2D) phased-array antenna steering. We present the integrated circuit design in Section 4.A. Finally, we discuss the development of the critical elements, wavelength- and bias-tunable slow-light waveguides, in Sections 4.B and 4.C, respectively. The significant size advantage of the integrated system will allow for deployment onto small radar platforms, such as unmanned aerial vehicles (UAVs).

2. PRINCIPLE CONCEPT AND ARCHITECTURE DESIGN

A. Design Concept

In a typical 2D phased-array antenna system, there are N elements in each row with identical spacing between elements, which is approximately half of the wavelength, and M elements in each column with the same spacing between columns. A beamforming device needs to program an appropriate phase delay or time delay for each element in order to steer the collimated beam to point one direction or angle in space; therefore, there are $N \times M$ parameters to program. For optical TTD array generators, it has to generate all the discrete time delays needed between any antenna elements. For each steering angle, these generators must create the appropriate optical path to generate the correct delay for each channel, hence increasing the complexity of the system. The complexity can be reduced by the described simple architecture implemented in this paper. For a phased-array antenna with equidistant emitter patches, only one variable, time delay ΔT_x between two adjacent elements, is needed, as shown in Fig. 1. Cascading the ΔT_x delay for the elements in each dimension results in integer multiples of the base delay $\Delta T_x, 2\Delta T_x, 3\Delta T_x \ldots N\Delta T_x$, achieving steering with a single variable. Therefore, for a 2D steering phased-array antenna system, it is able to reduce the $N \times M$ control parameters to only two variables ($\Delta T_x, \Delta T_y$) in the control system.

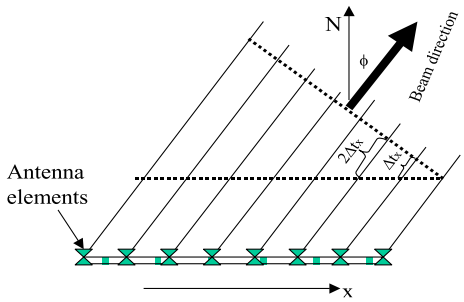

Fig. 1. Illustration of a 1D phased-array antenna. A ΔT_x emission delay between each antenna element causes a beam steered at an angle of Φ.

B. Earlier Work with a Free-Space Optics-Based TTD Generator

To demonstrate this concept, we first designed an optical TTD generator in free-space optics controlled by a linear displacement mechanical drive [14]. This TTD unit uses a zig-zag right-angle reflection mirror/splitter pairs that can automatically duplicate the ΔT_x time delay created between the first mirror pair by N times at the Nth optical output with TTD of $N\Delta T_x$. The delay can be directly tapped with the desired power distribution, such as a Chebyshev array for the Nth optical output. Therefore both amplitude and phase beamforming can be realized.

We built a 16×4 element array antenna system, as shown in Fig. 2. The antenna is designed for 3 GHz central RF frequency. We have demonstrated a −45 degree to +45 degree beam steering in a microwave anechoic chamber. The upper portion in Fig. 2 shows selected antenna patterns data from the experiments. A Dolph-Chebyshev array power distribution was realized for the 16 channels, which showed some side lops reduction in the antenna patterns [15].

However, this mechanical displacement mirror system limits the antenna steering speed; therefore, we subsequently replaced this free-space optical system with a fiber-optic-based system [16].

C. Design of the TTD Array Generator Using Fiber-Optic Devices

The variable relative delay time is made by tuning the optical wavelength for the laser transmitting through a fiber Bragg

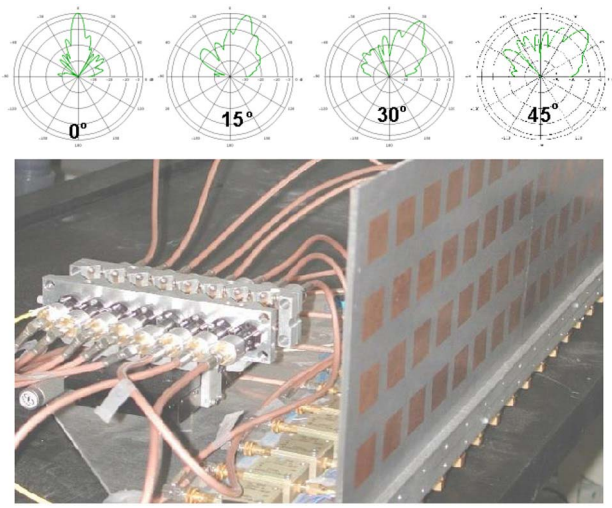

Fig. 2. Phased-array antenna with free-space TTD generation. Top: data of measured antenna patterns at various steering angles. Bottom: 16 × 4 phased-array antenna with free-space TTD generator.

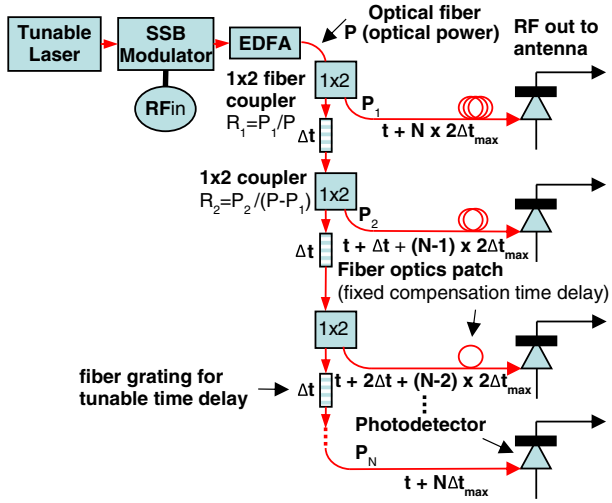

Fig. 3. Fiber-optic TTD array generator architecture. Varying the optical wavelength alters the delay Δt induced in each fiber Bragg grating. Integer multiples of Δt are induced after each successive grating and then tapped out at each node via the 1 × 2 splitters. Fiber patches at each node compensate for differences in optical path length at a center wavelength.

grating near the grating band edge that has a near linear change in the group velocity (and group index) when the wavelength of transmission light is shifted. Therefore, one can generate a relative tunable time delay ΔT by tuning the wavelength of the laser. The RF signal can be carried by the laser light via an optical modulator. However, when a CW laser light of wavelength λ_L is modulated by an RF signal, it will create two sidebands, λ_{+s} and λ_{-s}; the two RF sidebands will travel at slightly different group velocity. To avoid this unwanted dispersion effect on the RF signal, a single-sideband electro-optical (SS-EO) modulator has to be used to modulate the laser. Let us use $\exp\{-i(\omega_L t - \omega_L n_L x/C)\}$ to represent the laser carrier signal and $\exp\{-i(\omega_s t - \omega_s n_s x/C)\}$ to represent the single sideband traveling in the fiber at position x. Here ω_L, ω_s are defined as the frequencies of the laser carrier and the sideband signal, respectively, and the RF frequency ω_{RF} is $\omega_L - \omega_s = \omega_{\mathrm{RF}}$. n_L and n_s are the group index at the laser wavelength and sideband wavelength, respectively. C is the speed of light. When the laser and sideband signals are mixed at a photodetector, we will obtain an RF signal at the detector's output: $\exp\{-i[\omega_{\mathrm{RF}} t - (\omega_L n_L - \omega_s n_s)x/C]\}$. If we shift the laser wavelength from λ_L to λ_L' where the fiber Bragg grating's group index changes nearly linearly such that $n_L' = n_L + \Delta n$, and $n_s' = n_s + \Delta n$, since ω_{RF} will be the same, the RF signal at the photodetector will be then $\exp\{-i[\omega_{\mathrm{RF}}(t - \Delta n x/C) - (\omega_L n_L - \omega_s n_s)x/C]\}$. As we can see, with the near-linear index approximation, this laser wavelength change will generate a time delay $\Delta T = \Delta n x/C$, which is true-time delay that does not depend on ω_{RF}.

Using such gratings, we have designed an all-fiber TTD array generator, as shown in block diagram Fig. 3 [16]. CW light from a wavelength-tunable laser is modulated by the RF input through a SS-EO modulator. The modulated light is amplified by an Er-doped fiber amplifier (EDFA) and sent into a 1 × 2 fiber splitter with appropriate splitting ratio. The low percentage output signal is sent to the photodetector (PD) to generate the RF output for the first antenna element via an optical fiber patch that provides a fixed compensation delay. The high percentage output signal is sent to the fiber grating and cascaded 1 × 2 fiber splitter-grating for the second antenna element, and cascaded to the next splitter, etc. All cascaded fiber gratings are identical. A central wavelength λ_o is chosen such that all the compensating optical fiber patches are adjusted to have all RF signals radiated from each antenna element in-phase, resulting in a steering angle of 0. By shifting the optical wavelength from the central wavelength, positive or negative ΔT_s between neighboring elements are created. The antenna can be steered with positive or negative angles. In comparison to other approaches, much fewer components/devices are required in this system.

By designing the appropriate splitting ratio for each 1 × 2 splitter, one can also form a Chebyshev power distribution array to reduce the sidelobes and improve the beam collimation for the phased-array antenna.

D. Design of a Single System for Both Transmit and Receive Operation

The architecture shown in Fig. 3 can be directly used for transmission mode antenna beamforming. The RF signal (either for Radar or communication) will be fed into the SS-EO modulator. The output RF signals from the photodetector array will be fed into the antenna elements with a TTD sequence generated by the optical system that controls the beam-steering angle.

It is more challenging to design the optical TTD generator array for receiving mode operation, especially for Radar applications in which the system is required to maintain very high SFDR with very low noise figure. Previous receiving systems designed by others require one EO modulator for each antenna element to convert the received RF signal to an optical signal in

order to perform optical TTD [12]. To be able to achieve high SFDR, expensive custom-made linear EO modulators have to be used, which add significant cost since thousands of modulators may be needed for a large array system. In addition, these linear RF photonic links are typically made with $LiNbO_3$ modulators using a coherent link approach, which is not suitable for semiconductor integrated photonic circuits. We have designed a transmit/receive switching system that uses a different approach for the phased-array antenna receiving operation to avoid these problems [17]. Our concept is that the RF photonic links in our photonic TTD system are used only for clean transmit RF waveform signal input or single-frequency local oscillator (LO) RF input. Therefore there is no SFDR issue in our optical system. For antenna receive mode operation, our optical TTD generator only generates an array of LO signals with appropriate time delay between each other. Each LO signal will be mixed with the corresponding received RF signal at each antenna element via a mixer to downconvert the RF signal into an intermediate frequency (IF) signal. As a result all the IF signals are in-phase.

As shown in Fig. 4, our system can be used for both transmit and receive operations. A series of electronic switches is used to switch between transmit and receive modes. In the transmit mode, the RF transmit waveform generated by a waveform generator is used to modulate the laser light through the SS-EO modulator. For a required steering angle, the optical TTD array generator generates an array of the transmitted RF signals with appropriate TTDs that feed into the antenna elements though the switch matrix in transmission position via high-power RF amplifiers. For the receiving operation, instead of feeding an RF transmission input signal to the EO modulator, we apply an LO signal and use the same optical TTD array generator to create an array of LO signals with TTDs that correspond to the receiving RF signals incident angle (which is the same as the transmission angle) to the antenna.

At each antenna element, a switch matrix is used so that the received RF signal is mixed with the corresponding LO signal with the programmed time delay at a RF mixer. Therefore, the phase delay from the received RF signal will be canceled by the delay of LO signal for the IF signal output. As a consequence, the IF signals for all elements are in-phase, which can be combined and sent to an analog-to-digital converter for digital signal processing.

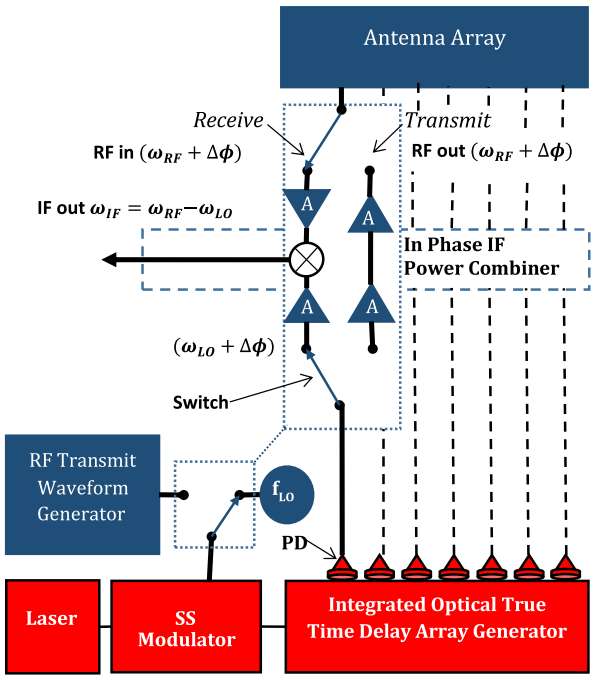

Fig. 4. Conceptual diagram for the optical controlled true-time-delay phased-array antenna for both transmit and receive operations.

E. Simultaneous and Independent Control of Multiple RF Beams

The tunable time delay line device made by a fiber Bragg grating or other "slow-light" dispersive device can be designed such that the dispersive region in which the group velocity changes is relatively narrow near the two outside band edges of the reflection band. Far away from these band edges, light will be transmitted without group velocity change. In this case, we can design an optical TTD array generator that can independently control multiple RF beams. Figure 5 shows the architecture for a fiber-optics-based optical TTD array generator for simultaneously controlling two RF beams independently.

Using two tunable lasers with wavelength λ_1 and λ_2, where the frequency difference between the two lasers is larger than the photodetector's bandwidth (such as >100 GHz), fed into two SS-EO modulators where the first RF beam signal f_1 is carried by laser λ_1 and the second RF signal f_2 is carried by laser λ_2, respectively. Both modulated laser lights are combined by a wavelength division multiplex combiner and sent to a series of cascaded 1 by 2 splitters and double fiber Bragg grating combinations. The double grating pair has a grating G1 which can generate a tunable time delay Δt_1 for λ_1 tuning, but is transparent without index change for λ_2, and vice versa; the second grating G2 generates Δt_2. At each photodetector both RF signals f_1 and f_2 will be sent to a corresponding antenna element and each has an appropriate true-time delay.

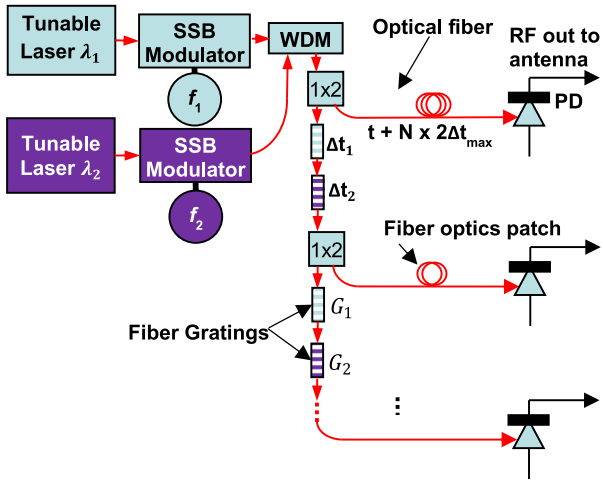

Fig. 5. Architecture of a two-beam fiber-optics-based optical TTD array generator for independent control of two RF beams in a phased-array antenna.

3. PROOF-OF-THE-PRINCIPLE EXPERIMENTAL DEMONSTRATION

A. Fiber Bragg Grating Design

Ordinary fiber Bragg gratings are designed for use in the reflection mode and there are rapid oscillations in dispersion near the band edge. To obtain smooth wavelength-dependent group delay, we have designed and modeled a long grating with high grating strength, a large number of periods, and Gaussian index profiled apodization. In previous work, we have described the theoretical modeling of the dispersion spectrum of fiber Bragg gratings [18]. Our final design involved using the fiber gratings in the transmission mode. The gratings were designed with index contrast apodized using Gaussian profiles (30%) near the end of the grating so as to have smooth power transmission and group delay profiles. This will improve the antenna performance by reducing beam fluctuations with laser wavelength tuning. Figure 6 shows a plot of the theoretical optical group delay versus wavelength dynamics of our fiber Bragg gratings [18]. Detailed treatments of Bragg grating dispersion theory can be found in many texts [19–21]. The simulation indicated that, with a 125 mm long grating, it is possible to obtain more than 100 ps relative time delay, which is needed to steer an X-band antenna beam by total 90 deg with −45 to 45 deg steering with respect to the normal incident angle.

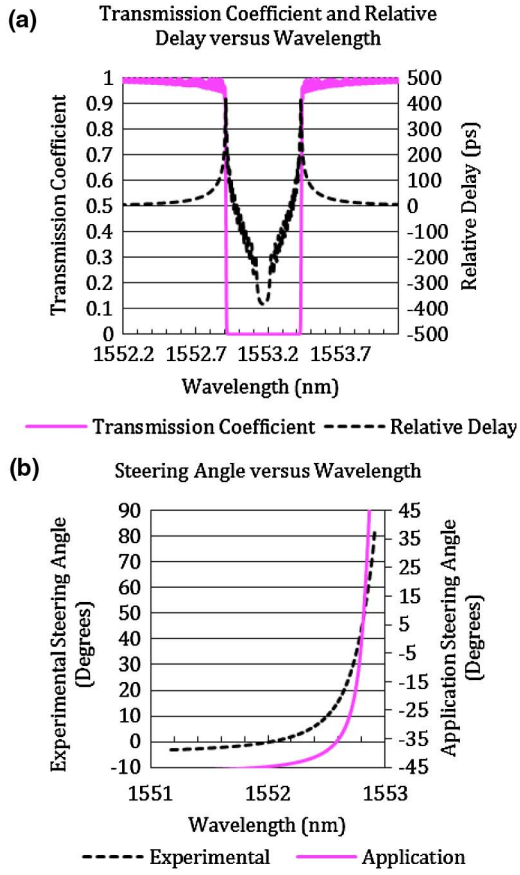

Fig. 6. Simulations of (a) group delay and transmission coefficient versus wavelength for a 125 mm long, index apodized fiber Bragg grating. (b) Predicted steering angle for different calibration wavelengths.

Recalling Fig. 1, the steering angle from normal follows a simple arctangent relationship between the emitter spacing (fixed at one-half wavelength, 15 mm, for 10 GHz) and the time delay between adjacent emitters. If one end of the tuning range was chosen as the wavelength corresponding to the normal steering angle, then one would need an infinite delay to achieve 90 deg steering. Figure 6(b) demonstrates that, by biasing the normal steering angle to occur at a wavelength in the middle of the tuning range, 90 deg tuning can be accessed with a finite delay. For the purposes of our proof-of-concept experimental demonstration, the normal emitting condition was calibrated for a wavelength of 1552.0 nm for convenience. This should allow the system to access ∼83 deg of steering angle, biased heavily the one direction. As an example for a future application, biasing of the normal emitting condition at 1552.8 nm, due to the nonlinear relationship between wavelength and relative delay, would instead allow for at least a full 90 deg sweep of steering angle, between ±45 deg. Experimentally, one can bias the normal incident angle and any wavelength in the Bragg grating's tuning range by an initial calibration process. This process involves adjusting the fixed fiber delay-line patch cords such that at the chosen wavelength, all the RF signals emitting at each antenna element are in-phase.

B. Experimental Demonstration of Fiber-Optics TTD Generator

We have designed and assembled an X-band, all-fiber-optic-based optically controlled phased-array antenna having a 30 × 4 element array, which is continuously steered one-dimensionally in the transmission mode. The phased-array antenna is assembled with the fiber-based TTD beamformer architecture shown in Fig. 3. A 10 GHz RF signal modulates a CW laser beam from a wavelength-tunable laser (Anritsu Model # 9638A) via a single-sideband lithium niobate optical modulator (CODEON part # 00001256010). The modulated beam is then amplified by an EDFA (Lightel part # EMH17C1C1) and then transmitted to the 29 cascaded fiber Bragg gratings and 1 × 2 fiber splitter pair time delay units, utilizing 29 near-identical fiber Bragg gratings custom made by Avensys (WO# 6289) as time delay elements. (The grating length is 125 mm, and the grating's center wavelength is 1553.17 nm.) The 1 × 2 fiber splitters are custom made by Lightel with designated power splitting ratio from 1% to 50% for these 29 splitters such that the optical power at each output node is nominally the same. At each node, the beam experiences a cumulative timed delay at a chosen wavelength λ_o, which represent the normal incident angle for the antenna. The output port of the 1 × 2 splitter of each node connects to a fixed fiber patch to compensate the fixed delay before reaching the corresponding photoreceiver (G-TRAN part # 550015), where a PD converts the optical signal back to an RF signal, which is then amplified by a transimpedance RF amplifier, and transmitted at the corresponding antenna element.

The length of each optical fiber delay line or patch cord cannot be made more precisely than a few millimeters; therefore, the true-time-delay array system must be first calibrated. For our experiment, we chose a center wavelength $\lambda_o =$ 1552 nm near the end wavelength tuning range of the system

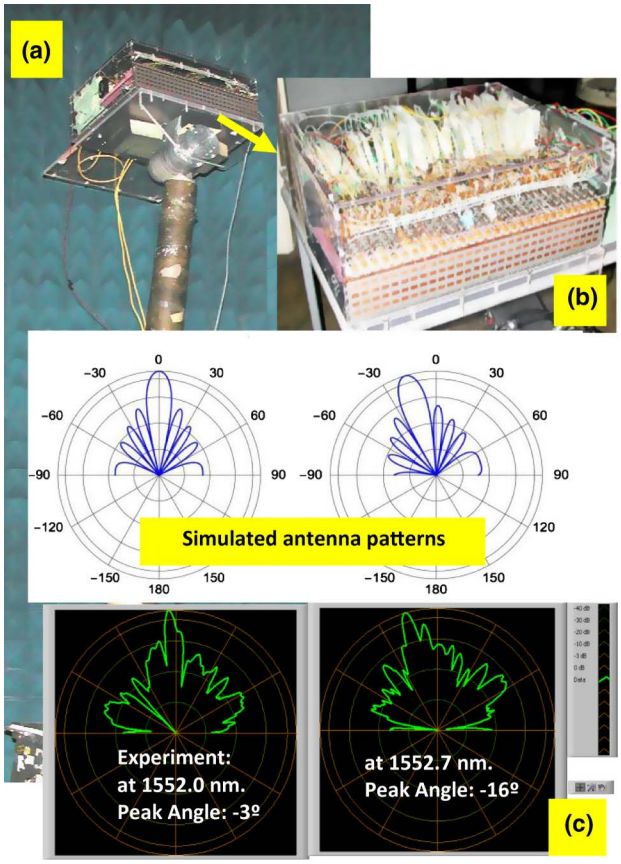

Fig. 7. Phased-array antenna experiment with the fiber-optic TTD generator: (a) measurement setup in anechoic chamber; (b) 30 × 4 phased-array antenna with fiber-optic TTD generator; and (c), top: calculated antenna patterns for 0 and −17 deg steering; bottom: experimentally measured antenna patterns at the two steering angles.

such that all outputs at the antenna are supposedly in phase so the steering angle is 0° from the normal direction of the phased array. This initial calibration involves that we need to adjust the fixed fiber patch cord length to bring the length error within one RF wavelength (about 20 mm) then add a RF waveguide phase trimmer at each RF output of the TTD generator to make the precise correction in the RF domain. Using an RF network analyzer, we can tune the RF phase trimmers to get all the output channels in phase. To measure the antenna pattern with different steered RF beam directions, we placed the phased-array antenna in an anechoic chamber and transmitted the beam, as shown in Fig. 7(a). By rotating the phased-array antenna and measuring the received power at the end of the chamber, we can determine the beam profile and direction relative to the plane of the antenna. We performed such measurements for several wavelengths near the central wavelength of our fiber Bragg gratings to steer the RF beam. We have simulated the antenna pattern using ideal phase (delay) and power distribution parameters. Figure 7(c) shows two selected experimental results of antenna patterns for azimuthal angles 0 and 17 deg, which are compared with corresponding predicted antenna patterns by simulation and calculation.

The results showed modest steering angle errors and sidelobes that were larger than theory predicted. This was caused by the slight angle alignment error when we placed the antenna in the chamber and the discrepancy in wavelength-dependent group delays and between the individually fabricated Bragg gratings and the theoretically calculated grating. Due to the grating manufacture's technical limitation, each of the 29 gratings are individually fabricated; the index contrast, apodization profile, etc., cannot be made exactly as we requested using our theoretical calculated parameter, and there is a small variation between the fabricated gratings. In addition, there are small index perturbations caused by temperature variation, fiber bending difference in the 29 packaged fiber gratings. These variations in the wavelength-dependent time (phase) delays of each emitting element resulted in an error of the beam steering angle, and increased sidelobes. Furthermore, the losses from the gratings and fiber connections made the power distribution of the array uneven, which causes larger than expected sidelobes. However, as a proof-of-concept experiment, the results clearly demonstrated the feasibility of using fiber Bragg gratings in transmission as time delay elements to build a simplified phased-array antenna architecture. We believe that with adequate engineering and packaging, this fiber-optics-based TTD array generator can be made inexpensively with more precision, uniformity and lower loss, thereby achieving satisfactory beamforming performance from this type of RF photonic phased-array antenna.

The shortfall of the fiber-optics-based TTD array generator is that each of the fiber Bragg gratings is at least 30 cm long with its fiber pigtails. For a large array system, a large number of these gratings have to be connected in series with one 1 × 2 fiber splitter between each consecutive grating. For each antenna element, a fixed compensation time delay line fiber has to be added; therefore, it became a system in large dimension with hundreds of fiber spools. In addition, the abovementioned fiber grating configuration can only steer the beam one dimensionally.

It is clear that if the fiber-Bragg-grating-based system can be replaced by a semiconductor-waveguide-based integrated circuit, all the problems, such as the lack of uniformity of the fiber Bragg gratings due to fabrication error and bending, large size, fiber length trimming error, etc., can be solved.

4. INTEGRATED PHOTONIC TTD ARRAY CIRCUIT FOR CHIP-SCALE BEAMFORMER FOR 2D PHASED-ARRAY ANTENNA STEERING

A. Semiconductor Integrated Photonic Circuit Design

In reality, the fiber-based TTD system was built only for the proof-of-concept demonstration purpose for the optical circuit architecture. Our ultimate goal is to develop a chip-scale semiconductor-based optical TTD beamforming/steering system for a large phased-array antenna system that can perform two-dimensional beam scan for both transmit and receive modes. This will enable a miniaturized optically controlled phase array antenna system to be used in a small platform such as UAV.

Figure 8 illustrates the block diagram of our conceptual semiconductor-based 2D array TTD generation system. It

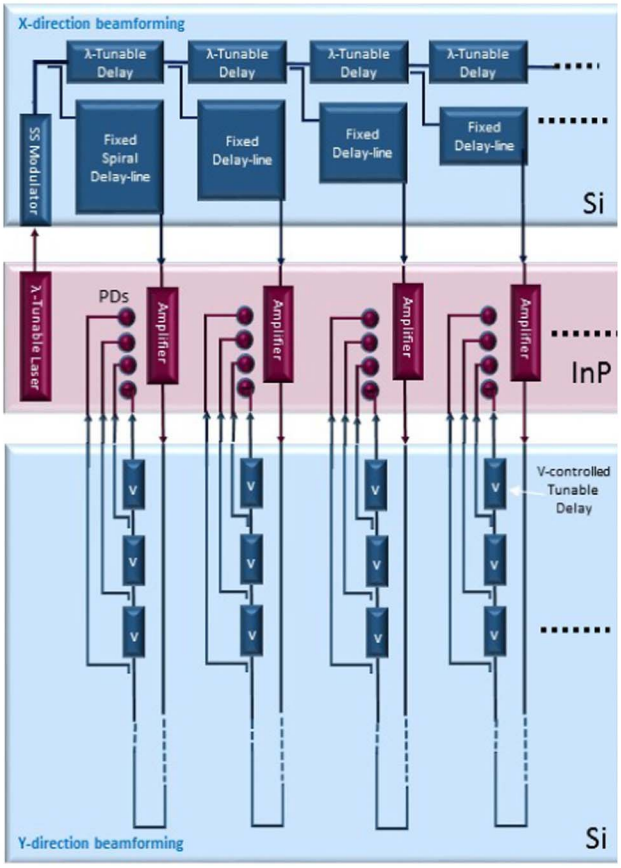

Fig. 8. Block diagram of integrated photonic chips for optical TTD generation of 2D phased-array antenna beamforming.

consists of three chips. The first one is a III-V semiconductor circuit chip that contains a tunable laser, optical amplifier array and photodetector array, as shown in the middle of the block diagram in Fig. 8. The second one shown on top of the diagram is a Si chip containing the waveguide delay-line array circuit for x-direction (horizontal) beamforming/steering. The third one is also a Si-based waveguide TTD generator array for y-direction (vertical) beamforming/steering, shown below the first chip. The output of a wavelength-tunable laser in Chip-1 is connected to the input of a single-sideband modulator input in Chip-2. The laser light is modulated by the RF signal (the RF transmission signal or LO signal for receiving mode) at the Si photonic single-sideband modulator. The modulated signal is sent to an optical TTD array generation circuit similar to the architecture shown in Fig. 3, except that the fiber gratings are replaced by a Si slow-light metastructure waveguide and the fixed fiber delays are replaced by regular low-loss waveguides.

Therefore N-channels of delayed signal ΔT_x, $2\Delta T_x$, $3\Delta T_x \ldots N\Delta T_x$ are created for N waveguide outputs for Chip-2 (without photodetectors). The variable ΔT_x is tuned by the wavelength of the input laser. The N waveguide outputs of Chip-2 are connected back to Chip-1 with N optical amplifiers on III-V material-based Chip-1. The N waveguide semiconductor optical amplifier outputs are fed to the N input ports on Si Chip-3, which has N Si TTD array generators for y-direction beamforming steering. Each of the y-direction TTD array generators also has similar cascaded tunable waveguide delay circuits, as shown in Fig. 3, again by using bias-tunable slow-light metastructure waveguides instead of fiber gratings. Therefore each TTD generator will generate an array of delayed signals ΔT_y, $2\Delta T_y$, $3\Delta T_y \ldots M\Delta T_y$ for one column of the 2D antenna array, where M is the total number of rows in the y-direction. Note that all the bias-tuned slow-light metastructure tunable delay waveguides are controlled by a single voltage bias for all N-columns of y-direction TTD array generators. Finally, all $N \times M$ waveguide outputs of Chip-3 are fed back to $N \times M$ photodetectors that can be placed in III-V Chip-1 that will be further integrated with a 2D patch antenna board that also contains a transmit/receive switching circuit with RF amplifiers, switches, mixers, etc., as shown in Fig. 4.

B. Wavelength-Tunable Slow-Light Waveguide

There are many semiconductor-based components in the proposed integrated photonic 2D beamforming circuits. Some of them are common devices that have already been developed, such as tunable lasers, semiconductor optical amplifiers, low-loss SiO_2 fixed delay-line waveguides, etc. However, the wavelength-tuned variable time-delay waveguides as well as the voltage-tuned time-delay waveguides are the two essential devices that need to be developed for these integrated photonic circuits. In this research effort, we focus on designing these tunable delay waveguides to achieve required time-delay tuning range and bandwidth with reduced device size.

Figure 9 shows the structure design of our tunable delay waveguide. We designed a silicon-based grating waveguide on a Si on insulator (SOI) substrate to generate wavelength-dependent delay ΔT_x for the x-direction of the 2D TTD array. The top view of the structure is shown in Fig. 9(a). To obtain a continuous tunable delay, super-Gaussian apodization is used to remove oscillations at the band edge [22]. Slow-light effect is observed in the wavelength range that is close to the band edge where the group index is sensitive to wavelength shift. The grating period Λ is chosen as 350 nm to set the band edge for transmission near $\lambda = 1.55$ μm. The width of the middle guided region of the waveguide (w) and the total width (W) including gratings are $w = 500$ nm and $W = 800$ nm, respectively. The thickness of the Si grating waveguide is 250 nm. SiO2 cladding layers are used for the calculation. The total length of the grating is 3.5 mm to obtain a total tunable delay of 60 ps.

The dispersion relation of the fundamental TE mode is calculated by the finite-difference time-domain (FDTD) method, using Lumerical FDTD Solutions, and plotted in Fig. 10. The dispersion curve exhibits a decreased slope as the frequency approaches the band edge, which indicates a higher group index $d\omega/dk$ region. The optical loss of the undoped grating waveguide is primarily due to material and fabrication imperfection.

The transmission spectrum and delay are calculated with couple-mode theory, and plotted in Fig. 11. As the apodization is properly designed, oscillation in the edge of the transmission window is eliminated. For wavelength tuning, the grating can provide a tunable delay of 17.1 ps/mm with a wavelength tuning range of ~1.1 nm from $\lambda = 1556.4$ to 1557.5 nm.

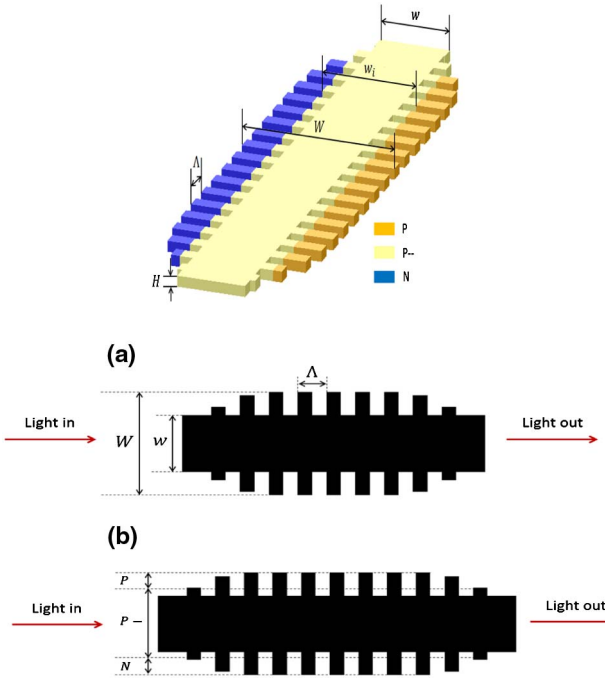

Fig. 9. Schematic of (a) a Si wavelength-tunable grating waveguide and (b) a bias-tunable grating waveguide using PiN structure.

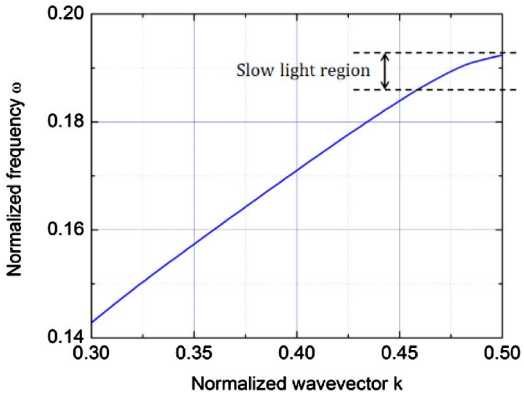

Fig. 10. Dispersion relation of the fundamental TE mode.

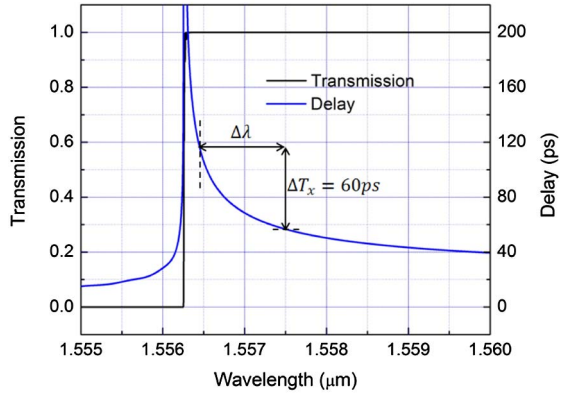

Fig. 11. Transmission and delay as a function of wavelength. The grating waveguide has a length of 3.5 mm.

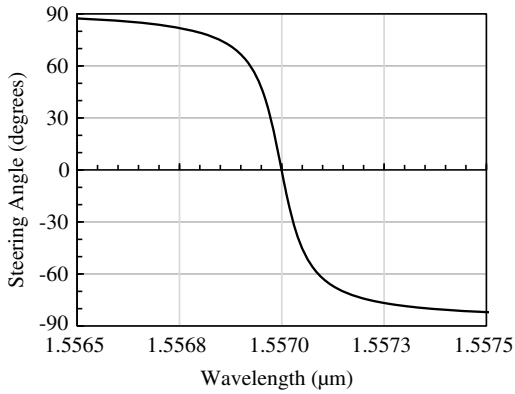

Fig. 12. Steering angle as a function of wavelength, for a grating of length 3.5 mm with an operation wavelength of 1.5570 μm, using a 30 GHz antenna.

The group index n_g is from 4.7 to 9.9 within this range. The steering angle as function of wavelength tuning is calculated for a 30 GHz (KA band) phased-array antenna by setting the operation wavelength at 1557.0 nm for the antenna radiation in the surface normal direction. A total delay of 60 ps will enable a total x-direction scan, shown in Fig. 12, which demonstrates that wide-angle steering is feasible within this wavelength range.

C. Bias-Tunable Slow-Light Waveguide

For the y-direction of the TTD array, a carrier-injection type of PiN structure is adopted to create continuous tuning by voltage bias. As illustrated in Fig. 9(b), the intrinsic region of the PiN diode is lightly doped to *P*- with a width of 600 nm. The diode has a doping concentration of NA $= 3 \times 10^{17}$ cm^{-3} in the *P* region, ND $= 1 \times 10^{17}$ cm^{-3} in the *N* region, and NA $= 3 \times 10^{16}$ cm^{-3} in the lightly doped *P*- region. The total length of the waveguide is 10.5 mm. The diode is operated in the carrier-injection mode. When the forward bias is tuned from 0 V to 1 V, a decrease in the effective index of $\Delta n = 0.001$ is obtained as a result of carrier injection to the waveguide. A blueshift in the transmission spectrum is observed, as shown in Fig. 13. A minimal delay tuning of $\Delta T_y = 25$ ps is obtained at $\lambda = 1557.5$ nm. This minimal delay tuning gives the

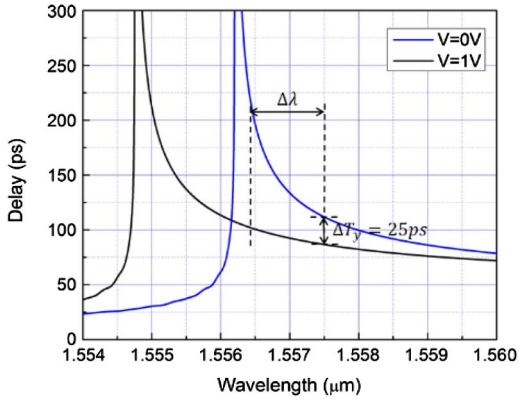

Fig. 13. Delay as a function of wavelength for $V = 0$ V and $V = 1$ V. The grating waveguide has a length of 10.5 mm.

worst-case available steering angle sweep. This ±12.5 ps delay about a central bias point corresponds to a steering angle sweep of ±82.4 deg for a 30 GHz antenna. The carrier-induced propagation loss is estimated to be negligible at 0 V and 1.67 dB/mm at 1 V due to free-carrier injection. A larger delay turning ΔT_y is expected for operation wavelength range closer to the band edge due to stronger slow-light effect. The optical loss can be reduced by using an operation wavelength range closer to the band edge so smaller forward bias or a shorter waveguide is needed to give the same ΔT_y due to the intensified slow-light effect. However, smaller wavelength operation range requires the laser source to have excellent resolution and very small spectral linewidth for precise control of delay tuning.

To integrate hundreds of these 3.5 mm wavelength-tuning slow-light waveguides and 10.5 mm bias-tuning waveguides along with fixed delay-line waveguides, it will still take a very large area on a Si chip. To further reduce these waveguides' lengths, we are investigating other types of high-contrast metastructure waveguides to increase the "slow-light" effect, therefore to achieve the same required delay with shorter device length [23,24].

5. CONCLUSION

We report our development of a photonic integrated true-time-delay array generation circuit for 2D phased-array antenna beamforming/steering using our simplified architecture. To demonstrate the concept of our simplified optical control of phased-array antenna architecture, we have first designed, fabricated, and experimentally tested a 1D steering optically controlled phased-array antenna using a fiber-optics-based system. The architecture uses a cascaded time delay approach with one laser/modulator without $1 \times n$ splitter and switches, significantly reducing the number of devices required in the system and having only one control variable (such as laser wavelength) for each dimension. The antenna has 30×4 elements operating at 10 GHz with 1D true-time delay array generation by an all-fiber-optic system.

This optically controlled phased-array antenna system is designed for both transmit and receive mode operation. We have carefully studied the RF system requirements so that a single optical system can meet those requirements for both transmit and receive modes.

We have also designed a multiple RF phased-array antenna system such that two or more RF beams can be controlled simultaneously and independently by the optical system.

In order to develop this simplified RF photonic beamforming architecture with semiconductor integrated photonic circuits, we have designed several Si-based waveguide devices as key elements of the integrated photonic circuit. This includes a slow-light waveguide, which can provide tunable time delays that be controlled by wavelength or voltage bias. This will enable a chip-scale phased-array antenna's beamforming units in the future.

Funding. U.S. Army Research Laboratory (ARL) Cooperative Agreement (W911NF-16-2-0049).

Acknowledgment. The authors thank Ms. Sholie Aina for her assistance as a summer student intern, and also thank Prof. Gary Carter and Prof. Jacob Khurgin for helpful discussions.

REFERENCES

1. R. J. Mailloux, *Phased Array Antenna Handbook* (Artech House, 2005).
2. M. Zatman, "Digitization requirements for digital radar arrays," in *Proceedings of the 2001 IEEE Radar Conference* (IEEE, 2001), pp. 163–168.
3. M. Mitchell and J. Fraschilla, "Digital beamforming subarray architecture for navy digital array radar (DAR)," in *Forty-Eighth Annual Tri-Service Radar Symposium*, Monterrey, California, 24–26 June 2002.
4. S. K. Garakoui, E. A. Klumperink, B. Nauta, and F. E. Van Vliet, "Phased-array antenna beam squinting related to frequency dependency of delay circuits," in *41st European Microwave Conference (EuMC)* (IEEE, 2011), pp. 1304–1307.
5. W. Ng, A. A. Walston, G. L. Tangonan, J. J. Lee, I. L. Newberg, and J. Bernstein, "The first demonstration of an optically steered microwave phased array antenna using true-time-delay," J. Lightwave Technol. **9**, 1124–1131 (1991).
6. E. N. Toughlian, H. Zmuda, and P. Kornreich, "A deformable mirror-based optical beamforming system for phased array antennas," IEEE Photon. Technol. Lett. **2**, 444–446 (1990).
7. R. D. Esman, M. Y. Frankel, J. L. Dexter, L. Goldberg, M. G. Parent, D. Stilwell, and D. G. Cooper, "Fiber-optic prism true time-delay antenna feed," IEEE Photon. Technol. Lett. **5**, 1347–1349 (1993).
8. J. L. Corral, J. Marti, J. M. Fuster, and R. I. Laming, "True time-delay scheme for feeding optically controlled phased-array antennas using chirped-fiber gratings," IEEE Photon. Technol. Lett. **9**, 1529–1531 (1997).
9. B. M. Jung, J. D. Shin, and B. G. Kim, "Optical true time-delay for two-dimensional X-band phased array antennas," IEEE Photon. Technol. Lett. **19**, 877–879 (2007).
10. H. Shahoei and J. P. Yao, "Delay lines," in *Wiley Encyclopedia of Electrical and Electronics Engineering* (Wiley, 2014), pp. 1–15.
11. A. Molony, C. Edge, and I. Bennion, "Fibre grating time delay element for phased array antennas," Electron. Lett. **31**, 1485–1486 (1995).
12. H. Zmuda, R. A. Soref, P. Payson, S. Johns, and E. N. Toughlian, "Photonic beamformer for phased array antennas using a fiber grating prism," IEEE Photon. Technol. Lett. **9**, 241–243 (1997).
13. C. H. Cox III, E. I. Ackerman, G. E. Betts, and J. L. Prince, "Limits on the performance of RF-over-fiber links and their impact on device design," IEEE Trans. Microwave Theory Technol. **54**, 906–920 (2006).
14. W. Zhou, "Simple true-time-delay generation for optical control of phased array antenna," U.S. patent 6,388,616 (14 May 2002).
15. W. Zhou and S. Weiss, "A low-cost optical controlled phased-array antenna with optical true-time-delay generation," Proc. SPIE **4998**, 133–138 (2003).
16. W. Zhou, "Electro optical scanning multi-function antenna," U.S. patent 7,609,971 (27 October 2009).
17. W. Zhou, "Electro optical scanning phased array antenna for pulse operation," U.S. patent 8,779,977 (15 July 2014).
18. O. Okusaga, W. Zhou, and G. Carter, "A tunable optical true time delay generator for phased array antenna," Proc. SPIE **6116**, 611608 (2006).
19. J. Skaar, "Synthesis and characterization of fiber Bragg gratings," Diploma thesis (Norwegian University of Science and Technology, 1997).
20. A. W. Snyder and J. D. Love, *Optical Waveguide Theory* (Chapman & Hall, 1983).
21. L. Poladian, "Resonance mode expansions and exact solutions for nonuniform gratings," Phys. Rev. E **54**, 2963–2975 (1996).
22. J. Zhao, "An object-oriented simulation program for fiber Bragg gratings," Doctoral thesis (Rand Afrikaans University, 2001).
23. W. Zhou, G. Dang, M. Taysing-Lara, and C. Chang-Hasnain, "Demonstration of a slow-light high-contrast metastructure cage waveguide," Proc. SPIE **8633**, 8633065 (2013).
24. L. Jiang, S. Anderson, H. Taleb, Z. R. Huang, and W. Zhou, "Active tunable high contrast meta-structure Si waveguide," Proc. SPIE **9757**, 97570G (2016).